THE
PHYSICAL REVIEW

A journal of experimental and theoretical physics established by E. L. Nichols in 1893

SECOND SERIES, Vol. 139, No. 4A 16 AUGUST 1965

Elastic Differential Scattering of He^+ Ions by He in the 20–600-eV Range*

DONALD C. LORENTS AND WILLIAM ABERTH
Stanford Research Institute, Menlo Park, California
(Received 22 March 1965)

Absolute elastic differential scattering cross sections for He^+ on He have been measured at relative energies of 20 to 600 eV over an angular range of 1–36°. The ions are extracted from an electron-bombardment source, formed into a ribbon beam by a pair of slits, and scattered in a gas cell containing He. The scattered beam is energy-analyzed and then detected by an electron multiplier. The relative data are normalized to absolute cross sections obtained at small angles using a Faraday cage in place of the multiplier. The effect of geometry, target-particle motion, and inelastic scattering on the angular resolution of the elastic cross sections is discussed. Three distinct interference phenomena are observed: (1) a series of smooth sinusoidal oscillations resulting from interference between the waves scattered from the *gerade* and *ungerade* potentials of the molecular ion, (2) rainbow scattering, (3) secondary oscillations at large angles due to nuclear interchange.

I. INTRODUCTION

ELASTIC and inelastic differential scattering cross sections measured over a wide range of angles and energies provide information which can lead to detailed understanding of two-body interactions. Such measurements have been used extensively in elucidating nuclear interactions but, with the exception of electron scattering, have only recently been seriously applied to the study of atomic interactions. Differential-scattering techniques have now become a popular method of determining interaction potentials and reaction mechanisms between neutral species of chemical interest.[1] Fedorenko and co-workers in the USSR[2] and Everhart and co-workers in the USA[3] have been largely responsible for extensive studies of ion-atom and ion-molecule interactions at small internuclear distances based on differential-scattering measurements. In the 1930's Ramsauer and Kollath[4] and Rouse[5] carried out a few low-energy ion-atom and ion-molecule scattering measurements, but no analysis of their experiments has been attempted. Though it is possible to do differential-scattering experiments with ions at very low energies with high angular and energy resolution, no concerted effort to use such measurements to derive information about ion-atom interaction potentials or excitation mechanisms has been made. Since approximate calculations of interatomic potentials for simple systems are possible it is essential to have experimental information with which to test such calculations.[6]

An extensive series of measurements of partial total scattering cross sections (the total scattering of particles at angles larger than some fixed angle) have been carried out for ions incident on various atomic and molecular species in the energy range of 5 to 5000 eV.[7] In an excellent review of these measurements, Mason and Vanderslice[7] describe the difficulties of extracting potential curves from the data provided by this type of experiment. In these integral-type experiments the measured cross section is an average over the radial intensity distribution of the beam and the scattering

* Supported in part by the Defense Atomic Support Agency through the U. S. Army Research Office (Durham) and Air Force Cambridge Research Laboratories.

[1] H. Pauly, Fortschr. Phys. **37**, 613 (1960); R. B. Bernstein, Science **144**, 141 (1964).

[2] N. V. Fedorenko, Zh. Techn. Fiz. **24**, 784 (1954); N. V. Fedorenko, Usp. Fiz. Nauk. **68**, 481 (1959) [English transl.: Soviet Phys.—Usp. **2**, 526 (1959)]; N. V. Fedorenko, L. G. Filippenko, and N. P. Flaks, Zh. Techn. Fiz. **30**, 49 (1960) [English transl.: Soviet Phys.—Techn. Phys. **5**, 45 (1960)].

[3] A brief account and a complete list of references of the Connecticut work is given in E. W. McDaniel, *Collision Phenomena in Ionized Gases* (John Wiley & Sons, Inc., New York, 1964).

[4] C. Ramsauer and R. Kollath, Ann. Physik **16**, 570 (1933).

[5] A. G. Rouse, Phys. Rev. **52**, 1238 (1937).

[6] A. Dalgarno, Rev. Mod. Phys. **35**, 611 (1963).

[7] E. A. Mason and J. T. Vanderslice in *Atomic and Molecular Processes*, edited by D. R. Bates (Academic Press Inc., New York, 1962), Chap. 17.

Copyright © 1965 by The American Physical Society.

path length. Potential functions with variable parameters are assumed and the parameters are determined from the measurements. A serious problem results from the impossibility of determining the uniqueness of the potential without *a priori* information. For these reasons, although a considerable number of accurate data are available, only very few have been used to establish interaction potentials.

In this and the following paper is described a joint experimental and theoretical effort on the He_2^+ system. We describe in this paper the measurement of differential cross sections for elastic scattering of 20–600-eV He^+ ions by He atoms in the angular range of about 1 to 36°. Marchi and Smith,[8] in the following paper, compare differential elastic cross sections calculated semiclassically from the best available potentials of He_2^+ with our measured cross sections.

Differential scattering measurements on the He^+-He interaction were first obtained by Ziemba and Everhart.[9] Their measurements of the electron-capture probability P_0 as a function of energy at a scattering angle of 5° demonstrated the resonant structure predicted by the impact-parameter theory.[10] Detailed measurements of P_0 as a function of angle from 0.4 to 4.4° in the energy range 0.4 to 250 keV have recently been reported by Lockwood, Helbig, and Everhart.[11] Everhart's[12] analysis of these data in terms of the simple two-state impact-parameter theory reveals a number of unexplained discrepancies. The most prominent disagreement is the result that P_0 does not oscillate between zero and one as predicted. Bates and McCarroll,[13] and Lichten[14] have indicated that damping effects in the elastic interaction will result from the participation of excited states in the collision. Detailed calculation for the H^+-H interaction by Bates and Williams[15] substantiates this hypothesis. Recently F. T. Smith[16] and F. J. Smith[17] have independently shown that damping will occur in the two-state problem without the involvement of higher states. In the course of our work a number of experimental "damping" effects have been uncovered and will be discussed in detail.

II. APPARATUS

The apparatus, shown schematically in Fig. 1 consists of two separately pumped vacuum chambers. Typical operating pressures in the main chamber are 1×10^{-7} Torr base pressure, 7×10^{-7} Torr with ion beam on, and 2×10^{-6} Torr with a gas in the scattering cell.

Beam ions are produced by electron bombardment. The 0.015-in.-diam tungsten filament provides adequate ($5\frac{1}{2}$-turn helix, about $\frac{3}{8}$ in. in diameter) emission at a current of approximately 11 A. Electrons, accelerated radially outward through the concentric grid and decelerated as they approach the extraction electrode, oscillate between the filament and the extraction electrode until they are collected on the grid. In helium, at an ion gauge pressure of 1.5 to 2.0×10^{-3} Torr and a grid filament potential difference of 90 V, a discharge occurs in the region of the grid with a subsequent grid current of about 300 mA. Helium ions thus produced are extracted axially to form a beam. Since the plasma potential of the discharge is approximately equal to the grid potential, the ion-beam energy is nearly equal to the grid potential plus the potential on the extraction electrode. The energy spread of the ion beam is of the order of 2 eV.

Since there is no mass analysis of the beam, it is necessary to produce the ionized helium with as low an electron bombarding energy as possible. At the minimum grid-filament potential difference of 90 V necessary to maintain a stable discharge, the production of He^{2+} is estimated at less than 0.1%.[18,19] Production of about 1% of He^+ ($2^2S_{1/2}$) can also be expected.[20] The helium used contained less than 0.01% impurity.

The helium ions produced in the ion source chamber enter the main chamber through a rectangular 0.5×0.1-cm slit. A second beam-collimation slit of the same dimensions is located on the scattering cell, 28.6 cm from the source slit. These and all other slits are coated with Aquadag to reduce beam instability caused by charging of the slits. The turret scattering cell is constructed of three concentric cylinders. The innermost cylinder is fixed in position and contains the second beam-collimation slit. Two grooved plates, one of which contains a gas inlet and ion gauge, cap the cylinders on top and bottom. The outermost cylinder contains a 0.05×0.5-cm exit slit and rotates together with the energy analyzer and detector from 5° below the beam to 110° above it. Center sections of the cylinders are milled out to enable this rotation to take place without exposing the center of the cell to the outside vacuum except through the two slits. With this arrangement the scattering cell gas pressure, typically 5×10^{-4} Torr, can be maintaned at least 100 times the main chamber pressure. The scattering cell operating pressure is maintained well within the linear region of the dependence of scattering signal on pressure. The primary ion beam is monitored at angles larger than 7° by an

[8] R. P. Marchi and F. T. Smith, following paper, Phys. Rev. **139**, A1025 (1965).
[9] F. P. Ziemba and E. Everhart, Phys. Rev. Letters **2**, 299 (1959); F. P. Ziemba, E. J. Lockwood, G. H. Morgan, and E. Everhart, Phys. Rev. **118**, 1552 (1960).
[10] D. R. Bates, H. S. W. Massey, and A. L. Stewart, Proc. Roy. Soc. (London) **A216**, 437 (1953); O. B. Firsov, Zh. Eksper. i Teor. Fiz. **21**, 1001 (1951).
[11] G. Lockwood, H. Helbig, and E. Everhart, Phys. Rev. **132**, 2078 (1963).
[12] E. Everhart, Phys. Rev. **132**, 2083 (1963).
[13] D. R. Bates and R. McCarroll, Advan. Phys. **11**, 36 (1962).
[14] W. Lichten, Phys. Rev. **131**, 229 (1963).
[15] D. R. Bates and D. A. Williams, Proc. Phys. Soc. **83**, 425 (1964).
[16] F. T. Smith, Bull. Am. Phys. Soc. **9**, 411 (1964).
[17] F. J. Smith, Phys. Letters **10**, 290 (1964); F. J. Smith, Proc. Phys. Soc. (London) **84**, 889 (1964).
[18] W. Bleakney and L. G. Smith, Phys. Rev. **49**, 402 (1936).
[19] P. T. Smith, Phys. Rev. **36**, 1293 (1930).
[20] W. E. Lamb and M. Skinner, Phys. Rev. **78**, 539 (1950).

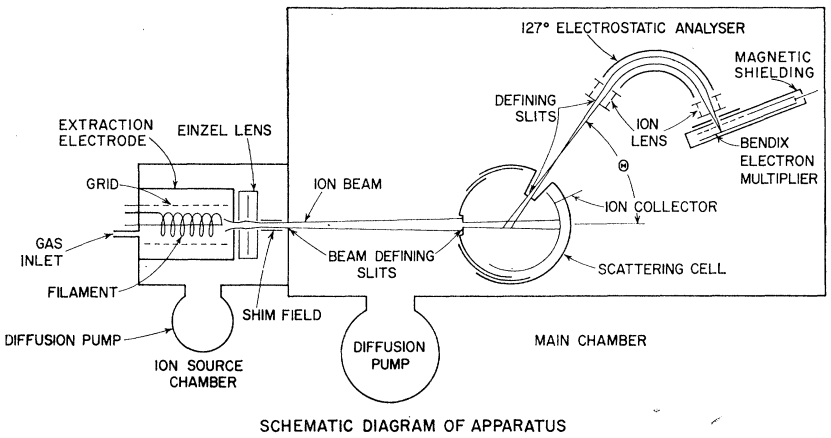

FIG. 1. Schematic diagram of apparatus.

ion collector plate located inside the scattering cell and mounted on the outermost cylinder.

The scattered ion beam is energy analyzed with a 127° cylindrical electrostatic analyzer of mean radius 5.5 cm. The entrance slit of the analyzer, which is the second collimating slit of the scattered beam, has dimensions of 0.05×1.0 cm and is 11.7 cm from the first collimating slit. The analyzer exit slit has dimensions 1.0×0.2 cm. The theoretical energy resolution is about 8% of the beam energy and is sufficient to resolve elastic from inelastic scattering at all ion energies used in this experiment (see Fig. 2). The analyzer constant, determined from the mean radius, allows the absolute beam energy to be calculated from the potential across the plates.

A Bendix M-306-1 magnetic electron multiplier coupled with a Cary 31 vibrating reed electrometer is used for ion detection. This combination enables signals of as low as 100 ions per second to be readily measured.

The energy analyzer, scattered beam slits, and electron multiplier are mounted on a rotatable platform whose axis of rotation coincides with the axis of the gas cell. The outermost cylinder of this cell, on which the first scattered beam slit is mounted, rotates together with the platform. The incident and scattered beam slits are optically aligned with the analyzer at 0°.

A 15-turn potentiometer geared to the rotational drive mechanism provides an output voltage proportional to the scattering angle. This signal and the output signal of the electrometer are supplied to a Leeds and Northrup two-pen recorder. A continuous simultaneous record of the scattered beam signal and the scattering angle is thereby produced.

III. EXPERIMENTAL PROCEDURE

The experimental values for the differential scattering cross section may be obtained from the equation[21]

$$\sigma(\theta) = I(\theta)\left[I_0 n \int_{\Delta X} \omega dx\right]^{-1}. \quad (1)$$

[21] Reference 3, p. 20.

In this equation $I(\theta)$ is the measured ion current scattered into the detector set at angle θ, I_0 is the incident ion current, n is the atom density in the scattering

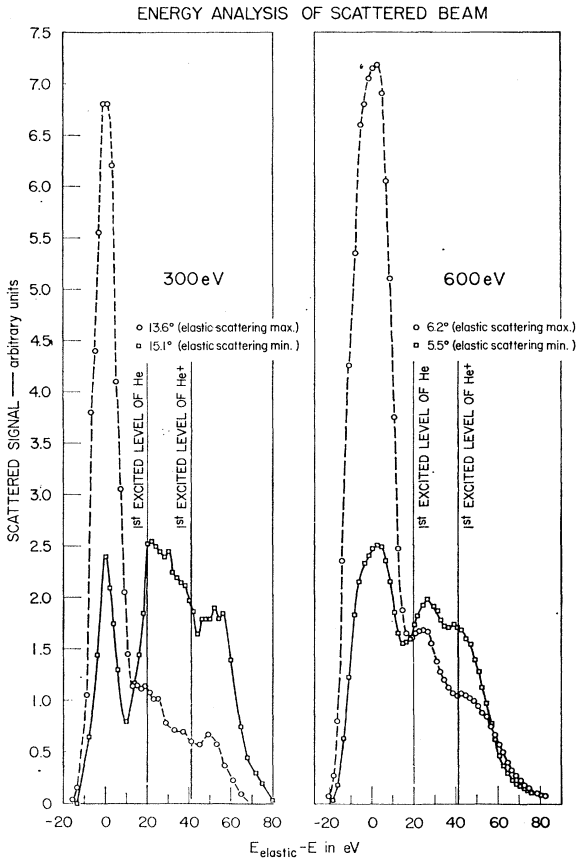

FIG. 2. Energy analysis of scattered He^+ ions at two angles, each for 300- and 600-eV incident energy. The abscissa is the difference between the energy of the elastically scattered ions at a given angle and the mean energy accepted by the analyzer and to good approximation equals the excitation energy. The decrease in energy resolution at the higher energy is a characteristic of the analyzer, but the resolution is sufficient to effectively separate the elastic from the inelastic scattering. The double-hump structure of the inelastic component is characteristic of all the inelastic scattering we have observed.

region, and $\int_{\Delta X} \omega dx$ is the geometrical factor obtained by integrating the scattering solid angle ω as seen by an element dx of the primary beam path along $\Delta X(\theta)$, the total length along the beam path that will contribute to the scattering signal. This integral may be approximated by[22]

$$\int_{\Delta X} \omega dx \cong \frac{abh}{d(d+l)\sin\theta}, \tag{2}$$

where a is the scattering-cell exit-slit width, b and h are the width and height of the analyzer entrance slit, d is the distance between the slits, and l is the distance from the scattering-cell exit slit to the center of the scattering cell. For our geometry this approximation is good to within 1% for angles larger than 1°.

The general procedure for obtaining a relative scattering cross section as a function of angle is as follows. With the electrostatic analyzer set at zero degrees to accept the incident beam, the analyzer potentials are adjusted for the desired energy and the beam intensity is optimized by adjustment of the ion source electrode voltages and the angular position of the analyzer. The angular position of the incident beam agrees with the optical alignment position for beam energies above 100 eV. At lower energies slight shifts in position are usually observed, but the zero angle position is accurately determined by sweeping through the beam. The analyzer is set in continuous rotational motion and a recording of the scattering signal and angular position is obtained. Since the energy of the elastically scattered ions is proportional to $\cos^2\theta$, the analyzer potential must be adjusted accordingly as the run proceeds. The recorded data are processed by drawing a smooth curve through the average of the signal noise, reading the values at small angular intervals, multiplying by the $\sin\theta$, and replotting.

In order to obtain absolute cross section measurements, all the factors of Eq. (1) were evaluated. For beam energies equal to or greater than 100 eV the following procedure was adopted. A simple Faraday cage collector was placed immediately behind the analyzer entrance slit (second defining slit for scattered beam) and the current collected, $I(\theta)$, was measured directly by an electrometer. By use of Eq. (2), the geometry factor was determined from measured values of the parameters. I_0 was obtained by means of the ion collector inside the scattering cell. The atom density n inside the scattering cell was measured with an ion gauge, calibrated directly by a McLeod gauge. Background noise in the Faraday cage prevented absolute measurements beyond six or seven degrees. A discussion of the procedure for normalization of the relative to the absolute data is given in Sec. IV.

At energies below 100 eV, large background noise and small scattering signal prevented absolute calibration by the above technique. Instead, the ratio of the multiplier output current at 3° scattering angle to full beam (0°) is compared to the same ratio obtained from the 100 eV relative data. This comparison gives the low energy cross section at 3 deg relative to that at 100 eV. Hence, once the 100-eV data are calibrated absolutely, the lower energy curves can be made absolute. This calibration procedure was checked by comparing the ratio of the 3° signal to the full beam signal for higher energy relative data with that of the 100 eV relative data. The higher energy absolute cross sections obtained by this technique were then compared with the absolute cross sections obtained directly from Eq. (1). The agreement between the two methods was consistently within 5%.

IV. ANGULAR RESOLUTION

The effective angular resolution of this experiment is determined by several factors. Because of the rapid variations of the cross section as a function of angle, it is important to consider all of these factors and as far as possible determine their effect on the cross section measurements.

A. Finite Slit Dimensions

The use of slits rather than circular holes was dictated by the desire to observe large angle as well as low energy scattering where signals are small. Filippenko[23] has analyzed errors in cross section measurements due to nonzero slit width and has demonstrated a method of approximately accounting for them. He did not, however, analyze the effect of the slit length which causes more distortion of the cross section at small angles than the width. No proper treatment of this problem has been found in the literature.

In Fig. 3, a description is given of an arbitrary beam

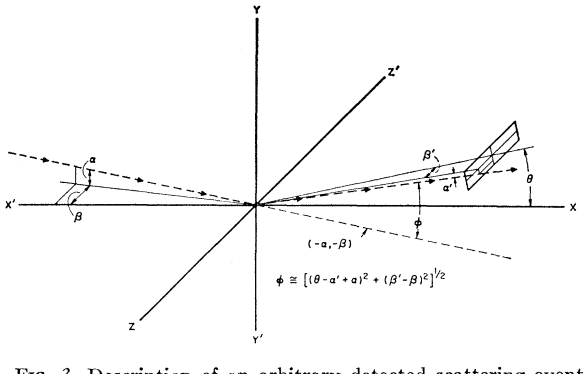

FIG. 3. Description of an arbitrary detected scattering event. The mean direction of the incident beam is along the X axis and α, β are small angle deviations from the mean direction. θ defines the mean direction of the scattered beam slits and α', β' are small angle deviations from it. φ is the actual scattering angle.

[22] E. B. Jordan and R. B. Brode, Phys. Rev. **43**, 112 (1933).

[23] L. G. Filippenko, Zh. Techn. Fiz. **30**, 57 (1960) [English transl.: Soviet Phys.—Tech. Phys. **5**, 52 (1960)].

particle which is scattered through angle φ and passes through the detector slits set at angle θ. The small angles, (α,β), (α',β'), designate, respectively, the directions of beam and scattered particle relative to the directions defined by each pair of slits. Let $P(\alpha,\beta)d\alpha d\beta$ be the distribution of beam particles over α and β. For a pair of identical slits $P(\alpha,\beta)d\alpha d\beta = P_1(\alpha)P_2(\beta)d\alpha d\beta$ where the P_1's are easily calculable triangular functions. Similarly, let $P'(\alpha'\beta')$ be the distribution of particles accepted by the detector slit pair. Then the probability for detecting an event such as that shown in Fig. 3 is

$$R(\theta,\alpha,\beta,\alpha',\beta') = P(\alpha,\beta)\sigma(\varphi)P'(\alpha',\beta')d\alpha d\beta d\alpha' d\beta', \quad (3)$$

where $\sigma(\varphi)$ is the differential scattering cross section and

$$\varphi \cong [(\theta-\alpha'+\alpha)^2+(\beta'-\beta)^2]^{1/2}. \quad (4)$$

The integral of this function over α, β, α', and β' gives the averaged cross section, $\langle\sigma(\theta)\rangle$, that is observed. The determination of $\sigma(\varphi)$ from the measured $\langle\sigma(\theta)\rangle$ is not easily accomplished. The above analysis is useful, however, for estimating the effective resolution limits due to the slits. From Eq. (4) it is seen that at large θ, both β and β' can be neglected, and therefore the slit widths determine the angular resolution. At small θ, the effect of the β's becomes more important as θ decreases. An effective angular resolution can be calculated for large angle scattering by evaluating the expression for $\langle\sigma(\theta)\rangle$ using a cross section which is independent of angle. For two pairs of identical slits, 92% of the detected particles are within $\pm\alpha_1$ of θ, the maximum angular deviation of one pair.

At small angles the problem is more difficult to analyze. We were fortunate to have available reliable calculated cross sections[8] for evaluating $\langle\sigma(\theta)\rangle$. The smearing effect of the slit height on calculated cross sections at 100 to 600 eV was calculated by numerical integration of Eq. (3) and the 100 eV result is shown in Fig. 4. In this calculation delta functions were used for $P(\alpha)$ and $P(\alpha')$ so that only the smearing effect of the slit length is obtained. The relative and absolute geometries differ in that the second slit of the detector pair is effectively longer for the absolute measurements. In the relative geometry the length of the second slit was limited by an aperture of the exit of the analyzer. It should be noted that not only is the smearing angular-dependent, but the peaks are shifted toward smaller angles and the cross section is lowered, particularly in the region between 1 and 2 deg where it is rising rapidly. These effects are observed in the experimental data shown in Fig. 5. Thus these calculations indicate how the relative cross section data should be normalized to the absolute data.

The finite resolution due to slit dimensions is probably responsible for the observed damping of the oscillations at small angles. Clearly, the finite resolution reduces the peak heights and raises the valley depths at all angles, but at angles above about 6° the regular oscillating structure is well resolved.

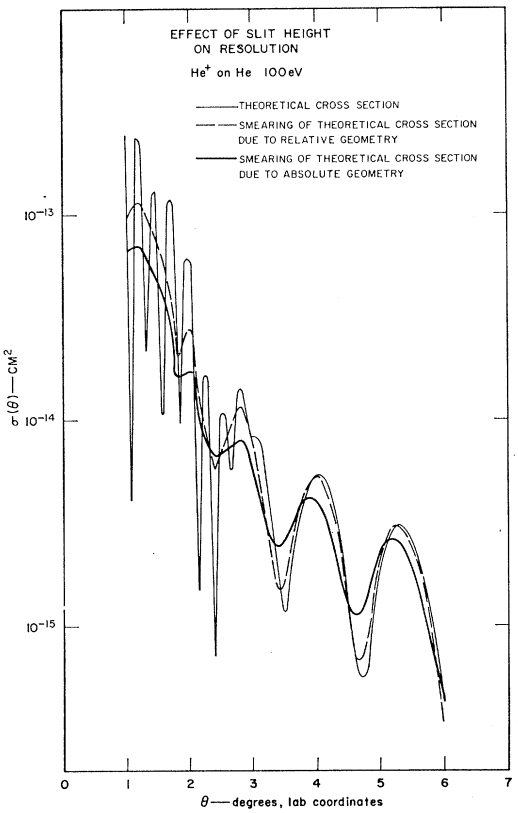

FIG. 4. Smoothing of the differential cross section at small scattering angles due to the use of a ribbon beam and long slits. The second detector slit in the absolute geometry was approximately twice the effective length of the slit used in relative geometry.

B. Thermal Motion of the Target Particles

Another source of smearing of the differential cross section which is particularly important at low incident energies is the velocity distribution of the target atoms. As a result of this motion, the center-of-mass velocity vector for a given incident energy is not constant for all collisions but has a distribution in direction and magnitude. For example, the angular distribution of center-of-mass velocity vectors for 100-eV He^+ ions incident on He atoms at 300°K is of the order of $\pm 1°$. Thus a given center-of-mass scattering angle will be seen in the laboratory system distributed over a range of angles. A general formulation of this problem has been given by Russek[24] who has worked out a number of examples. Unfortunately, he did not examine the experimentally interesting case of a cross section rapidly varying as a function of angle.

As in the case of the smearing due to the slit geometry, the problem of unfolding the center-of-mass cross

[24] A. Russek, Phys. Rev. **120**, 1536 (1960).

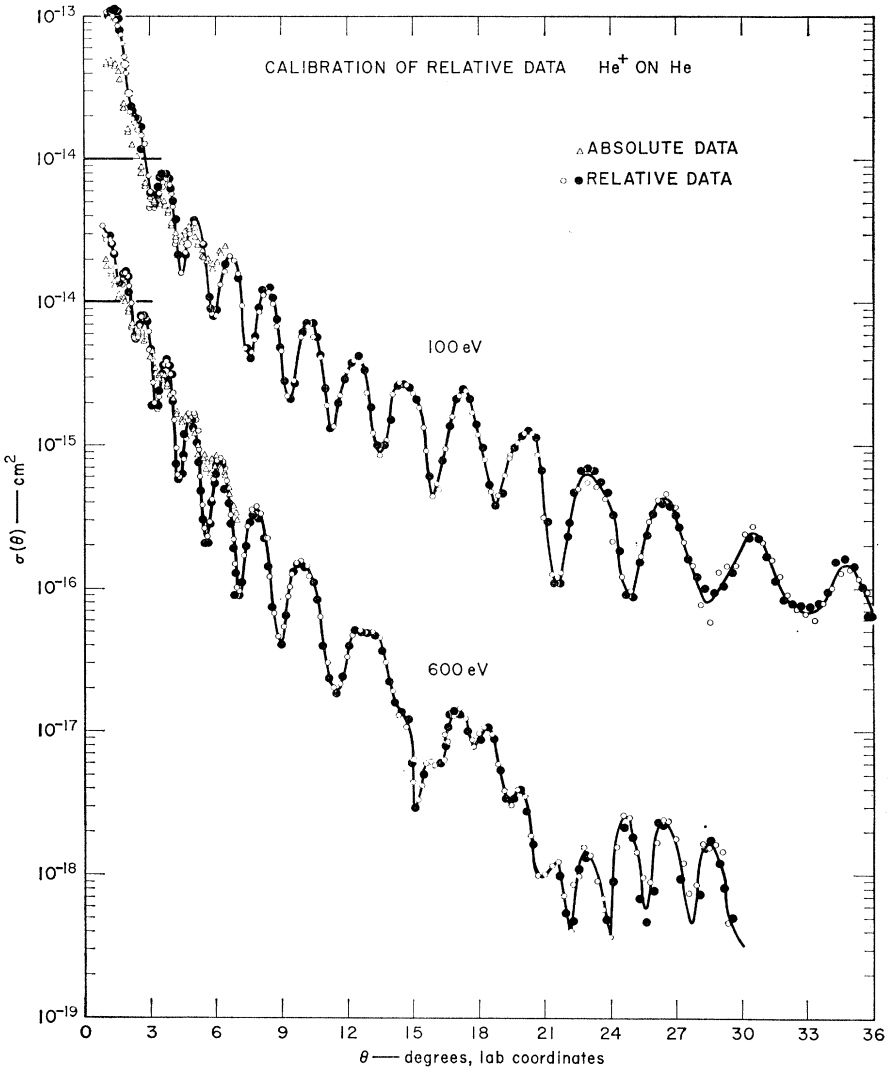

FIG. 5. Exemplary data at 100 and 600 eV showing data points with a smooth curve drawn through them. Note the shifted scale; the proper scale for each curve is identified at 10^{-14} cm² by the intersection of a horizontal line with each curve. The absolute data to which the relative data are normalized are also shown.

section from the measured cross section is intractable. However, a laboratory-observable cross section can be calculated for any given center-of-mass cross section.

C. Inelastic Scattering

The inelastic scattering in these collisions cannot be neglected. From the data given in Fig. 2, for example, it is observed that at the elastic scattering minimum at 15.1° and 300 eV the total inelastic component of the scattered beam exceeds the elastic component by a large factor. At 600 eV the inelastic component is obviously important at 5.5°. Since the inelastic scattering component varies smoothly with angle, it is essential to remove this component in order not to disturb the structure of the elastic scattering. In the apparatus used by Lockwood, Helbig, and Everhart,[11] no attempt was made to remove the inelastic component. Although they only studied the scattering at angles less than 5°, the energy range is sufficiently high to produce appreciable inelastic scattering at these angles. This effect may be responsible for some of the damping observed in their measurements.

V. RESULTS

Exemplary curves at 100 and 600 eV showing experimental points are given in Fig. 5. The relative data points are from single runs from zero to maximum angle and return. Absolute-cross-section data from two runs at each energy are also shown to illustrate the normalization of the relative data. The lower resolution of the absolute data is due in part to the effectively longer slit as well as to the inclusion of inelastically scattered particles. In the region of the elastic peaks the cross section is increased by less than 10% due to inelastic scattering and the effect is insignificant below 400 eV.

The reproducibility of the data points as shown in Fig. 5 indicates clearly that the nonsymmetries observed in many of the peaks and valleys, as well as the

subsidiary peaks, are intrinsic to the scattering events and cannot be attributed to scatter in the data. These curves have been reproduced several times under various operating conditions in an attempt to detect any structure in the curves due to the apparatus. The sensitivity of the irregularities to incident energy is additional evidence that the effects are not produced by the equipment.

The absolute magnitude of these cross sections is estimated to be accurate to $\pm 20\%$. This uncertainty arises from the absolute measurements which are accurate to $\pm 15\%$ and from the normalization which may be in error by $\pm 20\%$. The angular position of the cross section peaks at energies greater than 50 eV was reproducible to within 0.1° for angles less than about 8°, and to within 0.2° for larger angles. Below 50 eV the reproducibility was about 0.2° for angles less than 5°, and 0.4° for larger angles.

All of the elastic-differential-cross-section curves obtained from 20 to 600 eV are shown in Fig. 6. The structure in these curves exhibits three distinct features which we attribute to various interference phenomena. The prominent smooth oscillations of the cross section result from interference between the waves scattered from the lowest gerade and ungerade potentials describing the He_2^+ molecular ion. These are the oscillations predicted by the impact parameter theory and first demonstrated by Ziemba and Everhart.[9] The sharp increase of the cross section above the upper envelope of the oscillations which occurs at low energies as one proceeds toward small angles we attribute to rainbow scattering.[25] At large angles and high energies small oscillations are observed superimposed upon the major oscillations. As a result of the theoretical analysis in the following paper,[8] we attribute this structure to an interference occurring between the direct scattering of the incident ion at angle θ in the center-of-mass system and scattering with charge exchange at angle $\pi-\theta$. This interpretation has been experimentally verified by studying the scattering of He^{4+} by He^3.[26] Since nuclear exchange symmetry does not exist in this collision, the secondary oscillations are not expected to occur and, in fact, do not.

In Fig. 7 the angular positions of the maxima and minima of the scattering cross section are plotted as a function of energy. The data of Lockwood, Helbig, and Everhart obtained from measurements of P_0, the electron-capture probability, are also shown. The labeling is consistent with that of Everhart, since the maxima in the ion scattering correspond to minima in P_0. The discrepancies between our results and those of Lockwood *et al.* arise from two sources. Since the envelope of the scattering cross section is a steeply decreasing function of angle, the angles at which the peaks occur are shifted toward angles smaller than the peaks of P_0, and similarly the minima toward larger angles. In our small-angle data there is a noticeable pairing of the curves due to this effect. The second source of discrepancy is a general shift of the cross section curve toward smaller angles due to the slit effect discussed in Sec. IV A.

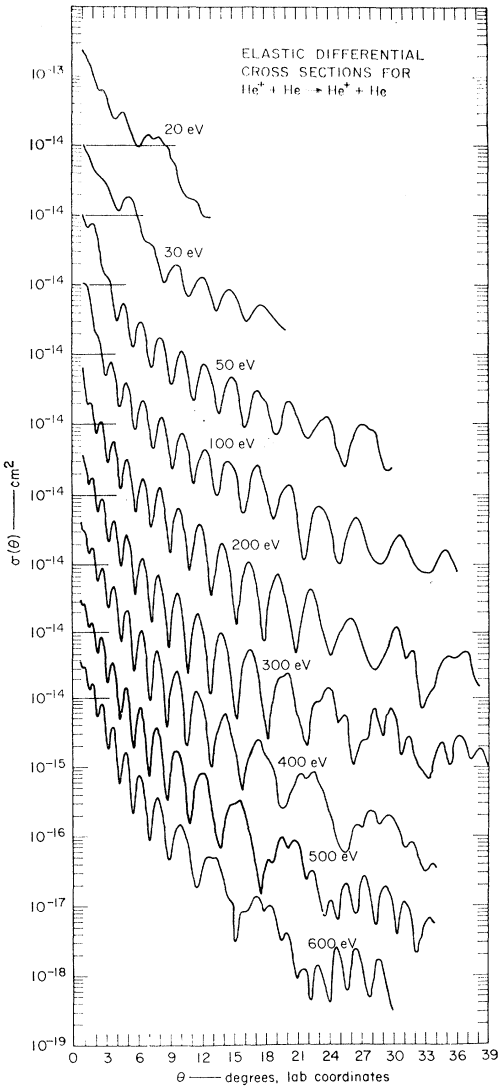

FIG. 6. Elastic differential scattering cross sections for He^+ on He at incident energies from 20 to 600 eV. Note the shifted scale; the proper scale is identified at 10^{-14} cm² by the intersection of a horizontal line with each curve.

A detailed interpretation of these results based on the theory of scattering from a central potential is given in the following paper by Marchi and Smith.[8] This accurate treatment based on calculated interaction potentials is in good agreement with the experimental results. A detailed empirical analysis of the data therefore seems unnecessary and has not been carried out.

[25] K. W. Ford and J. A. Wheeler, Ann. Phys. 7, 259 (1959).
[26] W. Aberth, D. C. Lorents, R. P. Marchi, and F. T. Smith, Phys. Rev. Letters 14, 776 (1965).

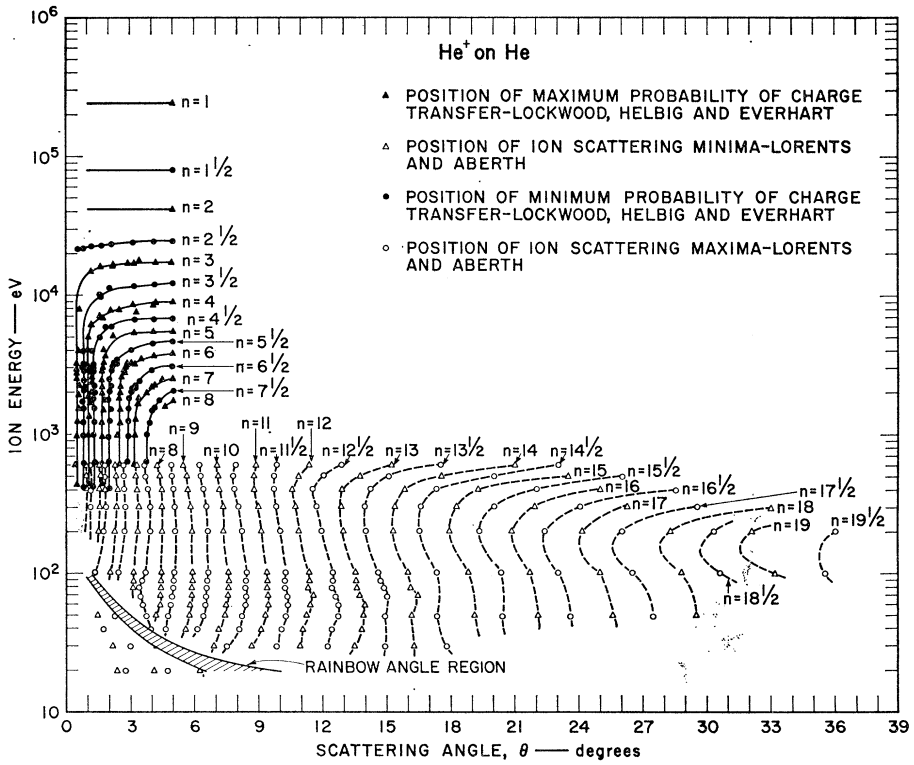

FIG. 7. Map of angular positions of cross-section maxima and minima as a function of energy. Data of Lockwood, Helbig, and Everhart (Ref. 11) are maxima and minima of charge-transfer probability.

It is noteworthy that inelastic scattering is observed at angles larger than 3° and energies above 100 eV. The inelastic component has not been studied in great detail, but it is observed, as expected, that harder collisions (large-angle scattering and high energies) result in more inelastic scattering. Our energy resolution is not sufficient to observe excitation of individual electronic states and therefore the inelastic signals we observe include a spectrum of states. Nevertheless, two broad peaks in the energy profile are observed in all the data we have obtained (see Fig. 2). The positions of these peaks on the energy scale suggest that the lower energy peak is due to excitation of the neutral atom and that the higher energy peak is due to excitation of the ion.

ACKNOWLEDGMENTS

We are indebted to our colleagues of the Molecular Physics Department, Dr. J. R. Peterson and Dr. C. J. Cook, as well as to Professor O. Heinz, U. S. Naval Postgraduate School, Monterey, for many valuable discussions concerning these measurements. The services of R. Leon and G. Conklin were invaluable to the successful construction and operation of the apparatus. We are deeply indebted to Dr. F. T. Smith and Dr. R. P. Marchi for much valuable guidance in the interpretation of the results.